BJP BRITISH JOURNAL OF PHARMACOLOGY

BPS BRITISH PHARMACOLOGICAL SOCIETY

British Journal of Pharmacology (2009), 158, 209–224

0007-1188/09
www.brjpharmacol.org

THEMED ISSUE: GPCR

RESEARCH PAPER

The $\alpha_{1B/D}$-adrenoceptor knockout mouse permits isolation of the vascular α_{1A}-adrenoceptor and elucidates its relationship to the other subtypes

L Methven, M McBride, GA Wallace and JC McGrath

Integrative and Systems Biology, Faculty of Biomedical and Life Sciences, West Medical Building, University of Glasgow, Glasgow, UK

Background and purpose: Mesenteric and carotid arteries from the $\alpha_{1B/D}$-adrenoceptor knockout ($\alpha_{1B/D}$-KO) were employed to isolate α_{1A}-adrenoceptor pharmacology and location and to reveal these features in the wild-type (WT) mouse.
Experimental approach: Functional pharmacology by wire myography and receptor localization by confocal microscopy, using the fluorescent α_1-adrenoceptor ligand BODIPY FL-Prazosin (QAPB), on mesenteric (an 'α_{1A}-adrenoceptor' tissue) and carotid (an 'α_{1D}-adrenoceptor' tissue) arteries.
Key results: $\alpha_{1B/D}$-KO mesenteric arteries showed straightforward α_{1A}-adrenoceptor agonist/antagonist pharmacology. WT had complex pharmacology with α_{1A}- and α_{1D}-adrenoceptor components. $\alpha_{1B/D}$-KO had a larger α_{1A}-adrenoceptor response suggesting compensatory up-regulation: no increase in fluorescent ligand binding suggests up-regulation of signalling. $\alpha_{1B/D}$-KO carotid arteries had low efficacy α_{1A}-adrenoceptor responses. WT had complex pharmacology consistent with co-activation of all three subtypes. Fluorescent binding had straightforward α_{1A}-adrenoceptor characteristics in both arteries of $\alpha_{1B/D}$-KO. Fluorescent binding varied between cells in relative intracellular and surface distribution. Total fluorescence was reduced in the $\alpha_{1B/D}$-KO due to fewer smooth muscle cells showing fluorescent binding. WT binding was greater and sensitive to α_{1A}- and α_{1D}-adrenoceptor antagonists.
Conclusions and implications: The straightforward pharmacology and fluorescent binding in the $\alpha_{1B/D}$-KO was used to interpret the properties of the α_{1A}-adrenoceptor in the WT. Reduced total fluorescence in $\alpha_{1B/D}$-KO arteries, despite a clear difference in the functionally dominant subtype, indicates that measurement of receptor protein is unlikely to correlate with function. Fewer cells bound QAPB in the $\alpha_{1B/D}$-KO suggesting different cellular phenotypes of α_{1A}-adrenoceptor exist. The $\alpha_{1B/D}$-KO provides robust assays for the α_{1A}-adrenoceptor and takes us closer to understanding multi-receptor subtype interactions.
British Journal of Pharmacology (2009) **158,** 209–224; doi:10.1111/j.1476-5381.2009.00269.x; published online 30 June 2009

This article is part of a themed issue on GPCR. To view this issue visit
http://www3.interscience.wiley.com/journal/121548564/issueyear?year=2009

Keywords: vascular smooth muscle; adrenoceptor; $\alpha_{1B/D}$-adrenoceptor knockout; wire myography; fluorescent ligand binding; confocal microscopy

Abbreviations: A-61603, N-[5-(4,5-dihydro-1H-imidazol-2-yl)-2-hydroxy-5,6,7,8-tetrahydronaphthalen-1-yl]methanesulphonamide; $\alpha_{1B/D}$-KO, $\alpha_{1B/D}$-adrenoceptor knockout; BMY 7378, 8-[2-[4-(2-methoxyphenyl)-1-piperazinyl] ethyl]-8-azaspiro[4.5]decane-7,9-dione; KO, Knockouts; QAPB, BODIPY FL-Prazosin; RS100-329, N-[(2-trifluoroethoxy)phenyl],N'-(3-thyminylpropyl) piperazine hydrochloride; SMC, smooth muscle cells; WT, wildtype

Introduction

Three genetically defined α_1-adrenoceptor subtypes (α_{1A}, α_{1B}, α_{1D}; nomenclature follows Alexander *et al.*, 2008) can produce similar cellular responses, including contraction of smooth

Correspondence: Dr L Methven, Integrative and Systems Biology, Faculty of Biomedical and Life Sciences, West Medical Building, University of Glasgow, Glasgow, G12 8QQ, UK. E-mail: l.methven@bio.gla.ac.uk
Received 7 November 2008; revised 30 January 2009; 23 February 2009

muscle (Guimaraes and Moura, 2001). Previous pharmacological work on α_1-adrenoceptor subtypes suggests that multiple subtypes are present in arterial preparations, causing the analysis of one subtype to be contaminated by the presence of the others (Daly *et al.*, 2002; Deighan *et al.*, 2005).

Little is known of the functional pharmacology of the three subtypes due to the similarity of their signalling, their widespread co-expression and the incomplete availability of selective pharmacological agents (Alexander *et al.*, 2008). This explains the conflicting pA_2 or pK_B estimates calculated by different groups using various assays for what is ostensibly the same subtype.

Little is known also of the location of the subtypes in native tissues. In cell culture, using epitope-tagged recombinant receptors, it has been proposed that through heterodimerization, the α_1-adrenoceptor subtypes might influence each other's cellular location and functional capabilities (Uberti *et al.*, 2003; Stanasila *et al.*, 2003; Hague *et al.*, 2004a,b). Through such approaches it has also been proposed that these receptor–receptor interactions might result in a different cellular distribution for each subtype. This relates to the concept that the α_{1B}-adrenoceptor is located mainly on the cell surface, while the α_{1A}-adrenoceptor and α_{1D}-adrenoceptor are mainly located at intracellular sites (Hirasawa *et al.*, 1997; Hrometz *et al.*, 1999; McCune *et al.*, 2000; Sugawara *et al.*, 2002). This is not a universal finding as, even in cultured cells, all three subtypes have been shown to be located both on the surface and at intracellular locations (Daly *et al.*, 1998; Hrometz *et al.*, 1999; Pediani *et al.*, 2000; Morris *et al.*, 2004).

There is, however, an alternative approach to studying α_1-adrenoceptor location, using the fluorescent ligand BODIPY FL-Prazosin (QAPB). This ligand has affinity for all three α_1-adrenoceptor subtypes (Daly *et al.*, 1998; Mackenzie *et al.*, 2000; Daly and McGrath, 2003; McGrath *et al.*, 2005). Because the α_{1A}-adrenoceptor spontaneously internalizes, when QAPB binds it is taken inside the cell and labels the receptor population in intracellular organelles; the receptors continuously recycle so that equilibrium is established between extracellular free ligand and the receptor population (Pediani *et al.*, 2005). This process can be blocked by subtype-selective competitor antagonists to identify subtypes in particular locations (Mackenzie *et al.*, 2000) and enables experiments in native tissue that are normally possible only in cell culture.

Normally in native tissues the presence of more than one receptor subtype complicates both pharmacological analysis and localization of receptors. However, mouse strains are available in which genetic knockouts (KO) of each α_1-adrenoceptor are present [α_{1A}-KO (Rokosh and Simpson, 2002); α_{1B}-KO (Cavalli *et al.*, 1997); α_{1D}-KO (Tanoue *et al.*, 2002b; Turnbull *et al.*, 2003)]. We have therefore pursued a strategy of isolating the α_{1A}-adrenoceptor in the double KO of the other subtypes ($\alpha_{1B/D}$-adrenoceptor knockout; $\alpha_{1B/D}$-KO). We employed a small artery, mesenteric first order, in which the α_{1A}-adrenoceptor is the major mediator of α_1-adrenoceptor-mediated vasoconstriction (Daly *et al.*, 2002; Martinez-Salas *et al.*, 2007) and where the other subtypes are expected to be modulatory (Daly *et al.*, 2002). A conductance artery, the carotid, was also examined to study a system in which the α_{1D}-adrenoceptor is the major mediator of α_1-adrenoceptor contractility but where an additional functional α_{1A}-adrenoceptor may exist (Deighan *et al.*, 2005).

The aim of this study was to use the $\alpha_{1B/D}$-KO to allow the study in native tissue of the remaining subtype, the α_{1A}-adrenoceptor, in respect of its pharmacological properties and cellular distribution and whether these change when it is isolated from the other α_1-adrenoceptor subtypes. We subsequently used this knowledge to try to understand the greater complexity that occurs when the other subtypes are present in the wild-type (WT) and to elucidate the possible interactions between subtypes.

Methods

Animals used and vessel preparation

All animal care and this investigation conformed to the provisions of the UK Animals (Scientific procedures) Act 1986. WT mice of C57BL6J/129Sv mixed background were used as controls for single knockouts of the α_{1B}-adrenoceptor (α_{1B}-KO), α_{1D}-adrenoceptor (α_{1D}-KO) and the $\alpha_{1B/D}$-KO. Mice were bred at the University of Glasgow from breeding pairs kindly provided by Professor Susanna Cotecchia (University of Lausanne, Lausanne, Switzerland; α_{1B}-KO) and Professor Gozoh Tsujimoto (National Children's Medical Research Center, Tokyo, Japan; α_{1D}-KO). $\alpha_{1B/D}$-KO were generated by cross-breeding the homozygous single KO mice at the University of Glasgow. The generation and background of the KO have previously been described in detail [α_{1B}-KO (Cavalli *et al.*, 1997); α_{1D}-KO (Tanoue *et al.*, 2002b); $\alpha_{1B/D}$-KO (Hosoda *et al.*, 2005)].

Mice were male weighing between 26 and 55 g [WT (26–47 g; $n = 74$); α_{1B}-KO (27–48 g; $n = 12$); α_{1D}-KO (26–42 g; $n = 12$); α_{1BD}-KO (26–55 g; $n = 80$)]. An earlier study showed that the predominant subtype present in hepatocytes could change between the commonly employed ages of 2–3 months (Deighan *et al.*, 2004), therefore the more mature 4–5-month-old mice were used. Mice were maintained on a 12:12 hour light/dark schedule at 22–25°C with 45–65% humidity and fed *ad libitum* on a standard rodent diet and provided drinking water. Mice were killed by carbon dioxide asphyxiation, and first order mesenteric and carotid arteries were isolated using a dissection microscope.

Experimental protocols for functional pharmacology

Two millimetre sections of artery were mounted in physiological salt solution on a four-chamber wire myograph (Danish Myotechnology, Aarhus, Denmark). Following a 30 min equilibration period, passive tension of 250 mg was applied to both types of arteries, and vessels were allowed to equilibrate for a further 45 min. Data were recorded by using Powerlab and Chart (version 5.0) (ADInstruments, Chalgrove, UK). Vessels were challenged with 10 μM of one of three agonists [the standard α_1-adrenoceptor agonist, phenylephrine; an agonist selective for the α_{1A}-adrenoceptor, A-61603 (N-[5-(4,5-dihydro-1H-imidazol-2-yl)-2-hydroxy-5,6,7,8-tetrahydronaphthalen-1-yl]methanesulphonamide) (Knepper *et al.*, 1995); or 5-hydroxytryptamine]. Acetylcholine (3 μM) was used to test the viability of the endothelium following preconstriction.

Cumulative concentration–response curves were produced for each agonist in half-log increments from 1 nM to 30 μM or 100 μM. Subtype-selective antagonists were incubated for 30 min: prazosin 1 nM, 10 nM and 100 nM (non-selective α_1-adrenoceptor antagonist); 5-methylurapidil 10 nM and 100 nM [α_{1A}-adrenoceptor-selective antagonist (Gross *et al.*, 1988)]; RS100-329 (N-[(2-trifluoroethoxy)phenyl],N′-(3-thyminylpropyl) piperazine hydrochloride) 1 nM, 10 nM and 100 nM [α_{1A}-adrenoceptor-selective antagonist (Williams *et al.*, 1999)]; BMY 7378 (8-[2-[4-(2-methoxyphenyl)-1-piperazinyl]ethyl]-8-azaspiro[4.5]decane-7,9-dione) 1 nM, 10 nM and 100 nM [α_{1D}-adrenoceptor-selective antagonist (Goetz *et al.*, 1995; Saussy *et al.*, 1996)]; or rauwolscine 10 nM (non-selective α_2-adrenoceptor antagonist).

Experimental protocols for visualization of smooth muscle cell α_1-adrenoceptors

QAPB incubations. 3–5 millimetre segments of mesenteric and carotid arteries were incubated with QAPB (100 nM) for 120 min. Live unfixed tissue was used to remain as faithful as possible to the *in vitro* state used to assess functional pharmacology. All incubations were performed at room temperature (21°C), and solutions were replaced every 30 min to maintain pH conditions.

Additional experiments using non-fluorescent antagonists to compete for QAPB binding sites were performed in segments from the same animals as QAPB controls (see Figure S1). Based on the timescale reported by Pediani *et al.* (2005), segments were incubated with QAPB for 60 min to establish an equilibrium, then co-incubated for a further 60 min with QAPB and an antagonist at 100 nM: prazosin, rauwolscine, RS100-329 or BMY 7378. The concentration of each antagonist was selected to be capable of competing effectively with QAPB at a specific α_1-adrenoceptor subtype but not at other potential binding sites based on pK_i estimates from the literature at the cloned α_1-adrenoceptor subtypes (Table 1). For instance, at α_{1A}-adrenoceptors, RS100-329 has higher affinity than QAPB, but at the α_{1B}-adrenoceptor or α_{1D}-adrenoceptor, its affinity is lower. Thus, used at the same concentration as QAPB (100 nM), RS100-329 should be capable of displacing QAPB from α_{1A}-adrenoceptors but not from other binding sites.

Slide preparation and image capture. Arteries were mounted in the incubation solutions with a coverslip (No. 1.5) on top. The thin-walled mesenteric artery was mounted intact, while the carotid artery was sliced open with a single-edged razor blade and laid flat (Miquel *et al.*, 2005) to optimize visualization through the luminal side of the thick arterial wall.

Optical sections were collected on a Bio-Rad Radiance 2100 Confocal Laser Scanning System at an excitation/emission of 488/515 nm for QAPB. Arteries were visualized by using ×40 oil immersion objective (NA 1.0). Optimal laser, gain and offset (contrast and brightness) were determined and then kept constant for each artery. Photomultiplier sensitivities were set such that all pixels fell within the range 0 (black) to 255 (white). Carotid arteries were imaged at high power (zoom 8) to include only smooth muscle cells and avoid areas containing elastic lamina in the media. Mesenteric artery images were collected at low power (zoom 3), which allows coverage of a wider area of exclusively smooth muscle cells. Arteries were scanned as 0.5 μm slices from the internal elastic lamina through the media producing Z-series in stacks of approximately 20–30 μm in depth. Each procedure was carried out in triplicate on four different mice per strain.

Data analysis and statistical procedures

All graphical and statistical analysis was performed by using Graph Pad Prism (version 5.0). Mean data were compared across mouse strains and also in the presence and absence of the selected antagonists using one-way ANOVA and Bonferroni's post test or Student's *t*-test.

Functional pharmacology. Data were expressed as a percentage of the control curve maximum and represents the mean value ± standard error of the mean. When a maximum response was achieved, pEC_{50} values were calculated for control curves and agonist curves in the presence of antagonists.

Quantitative confocal microscopy. Image analysis was based on the 2D image analysis as described by Miquel *et al.* (2005) and performed by using Metamorph software (version 4). In cell cultures fluorescent ligand binding follows similar kinetics to radioligand binding (Mackenzie *et al.*, 2000). However, the

Table 1 Ligand binding at α_1-adrenoceptors (AR) (mean pK_i for antagonists at cloned receptors)

Antagonist		*α_{1A}-AR*	*α_{1B}-AR*	*α_{1D}-AR*	*References*
Prazosin	Mean	9.6	9.8	9.7	1–3
	Range	9.0–9.9	9.0–10.3	9.0–10.0	
5-Methylurapidil	Mean	8.7	7.0	7.4	1, 4–10
	Range	8.3–9.2	6.1–7.4	6.1–7.9	
RS100-329	Mean	9.5	7.6	7.9	11–12
	Range	9.3–9.6	7.3–7.8	7.9–7.9	
BMY 7378	Mean	6.4	6.6	8.5	1, 4, 8, 12–17
	Range	6.0–7.1	6.2–7.5	8.1–9.3	
QAPB		8.7	8.4	8.1	1

1 MacKenzie *et al.* (2000); 2 Knepper *et al.* (1995); 3 Michel and Goepel (1998); 4 Saussy *et al.* (1996); 5 Goetz *et al.* (1994); 6 Leonardi *et al.* (1997); 7 Garcia-Sainz *et al.* (1995); 8 Yoshio *et al.* (2001); 9 Buckner *et al.* (1996); 10 Meyer *et al.* (1996); 11 Williams *et al.* (1999); 12 Deighan *et al.* (2004); 13 Goetz *et al.* (1995); 14 Kenny *et al.* (1995); 15 Testa *et al.* (1997); 16 Hieble *et al.* (1995); 17 Piascik *et al.* (1997).
BMY 7378, 8-[2-[4-(2-methoxyphenyl)-1-piperazinyl]ethyl]-8-azaspiro[4.5]decane-7,9-dione; QAPB, BODIPY FL-Prazosin; RS100-329, N-[(2-trifluoroethoxy) phenyl],N′-(3-thyminylpropyl) piperazine hydrochloride.

relationship between receptor number and fluorescence is not quantitatively established. Therefore, the measurement of ligand binding can be interpreted to identify which receptor subtypes are present but cannot be interpreted in terms of precise numbers of receptors. A single plane at a depth of 4–6 μm from the internal elastic lamina of each Z-series that captured only smooth muscle cells was selected for analysis. Average pixel intensity was measured for the entire plane (mesenteric artery 96 × 96 μm; carotid artery 36 × 36 μm). In addition, individual smooth muscle cells from each image were outlined as a Region of Interest to measure average pixel intensity (see Figure S2). It should be noted that this analysis was performed only on smooth muscle cells that showed fluorescent binding. The average pixel intensity correlated to a greyscale range of 0 (black) to 255 (white), with intermediate intensities being assigned an appropriate grey level.

Materials

Physiological salt solution composition (in mM): 119 NaCl, 4.7 KCl, 1.2 $MgSO_4.H_2O$, 1.2 KH_2PO_4, 24.9 $NaHCO_3$, 2.5 $CaCl_2$ and 11.1 glucose.

All analytical grade drugs were dissolved and diluted to the required concentration in distilled water (unless otherwise stated). Drugs supplied by Sigma Aldrich (Poole, UK) were phenylephrine, acetylcholine, 5-methylurapidil, prazosin, 5-hydroxytryptamine, BMY 7378; by Tocris(Bristol, UK) were A-61603, RS100-329, rauwolscine; and by Invitrogen (Paisley, UK) was QAPB (dissolved in DMSO and diluted in freshly gassed physiological salt solution).

Results

Functional pharmacology in mesenteric arterial rings

In the WT and all three KO strains, the maximum response and sensitivity to 5-hydroxytryptamine was similar (Table 2). This eliminates generic structural or smooth muscle sensitivity changes as a basis for differences subsequently found using drugs acting via α_1-adrenoceptors.

Cumulative concentration–response curves to the non-selective α_1-adrenoceptor agonist phenylephrine were obtained in all mouse strains [Figure 1A (data not shown for α_{1B}-KO and α_{1D}-KO)], with no significant differences between the WT and KO mice (Table 2).

The more selective agonist A-61603 was used to study the α_{1A}-adrenoceptor response. Concentration-dependent contractions were obtained to A-61603 in the WT and $\alpha_{1B/D}$-KO (Figure 1B). The maximum response was significantly higher in the $\alpha_{1B/D}$-KO than in the WT (Table 2). In both the WT and $\alpha_{1B/D}$-KO, sensitivity to A-61603 was significantly higher than to phenylephrine (Table 2) consistent with the α_{1A}-adrenoceptor being the main functional α_1-adrenoceptor in the mesenteric artery.

In both the WT and $\alpha_{1B/D}$-KO tissues, prazosin competitively antagonized the responses to phenylephrine (Figure 2A,B).

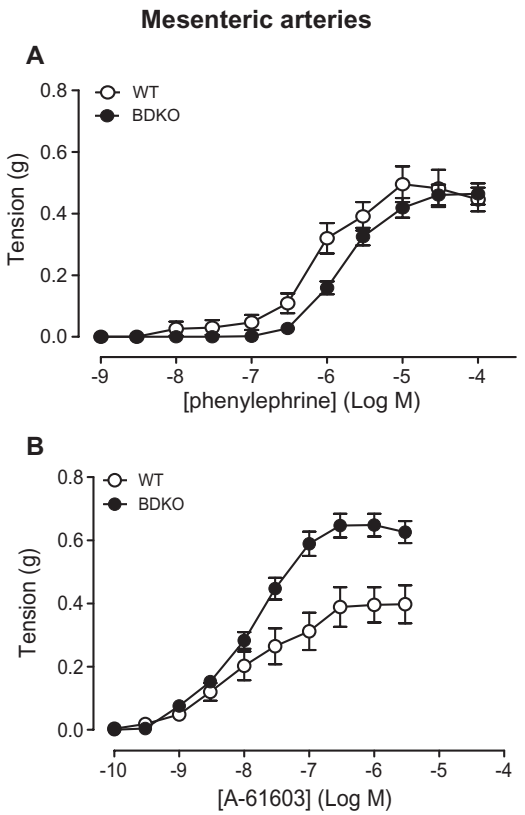

Figure 1 Contractile responses to (A) phenylephrine (n = 6) and (B) A-61603 (N-[5-(4,5-dihydro-1H-imidazol-2-yl)-2-hydroxy-5,6,7,8-tetrahydronaphthalen-1-yl]methanesulphonamide) (n = 7) in mesenteric arteries of wild-type (WT) and $\alpha_{1B/D}$-adrenoceptor knockout (BDKO) mice. Data points are expressed in g tension as mean ± SEM.

Table 2 Agonist responses in mouse mesenteric arteries

Mouse	*Phenylephrine*		*A-61603*		*5-Hydroxytryptamine*	
	Maximum response (g)	pEC_{50}	*Maximum response (g)*	pEC_{50}	*Maximum response (g)*	pEC_{50}
WT	0.52 ± 0.06	6.2 ± 0.08	0.41 ± 0.05	8.3 ± 0.11***	0.18 ± 0.04	6.9 ± 0.18
α_{1B}-KO	0.42 ± 0.07	5.8 ± 0.14	–	–	0.17 ± 0.04	6.9 ± 0.16
α_{1D}-KO	0.48 ± 0.05	5.9 ± 0.09	–	–	0.17 ± 0.02	6.8 ± 0.12
$\alpha_{1B/D}$-KO	0.49 ± 0.08	6.4 ± 0.17	0.66 ± 0.04**	8.0 ± 0.09***	0.19 ± 0.02	7.0 ± 0.13

Maximum responses and pEC_{50} values are expressed as mean ± SEM.
A-61603, N-[5-(4,5-dihydro-1H-imidazol-2-yl)-2-hydroxy-5,6,7,8-tetrahydronaphthalen-1-yl]methanesulphonamide; $\alpha_{1B/D}$-KO, $\alpha_{1B/D}$-adrenoceptor knockout mouse; WT, wild-type.
**P < 0.01 compared with WT (one-way ANOVA, Bonferroni's post test).
***P < 0.001 compared with phenylephrine-induced response (one-way ANOVA, Bonferroni's post test).

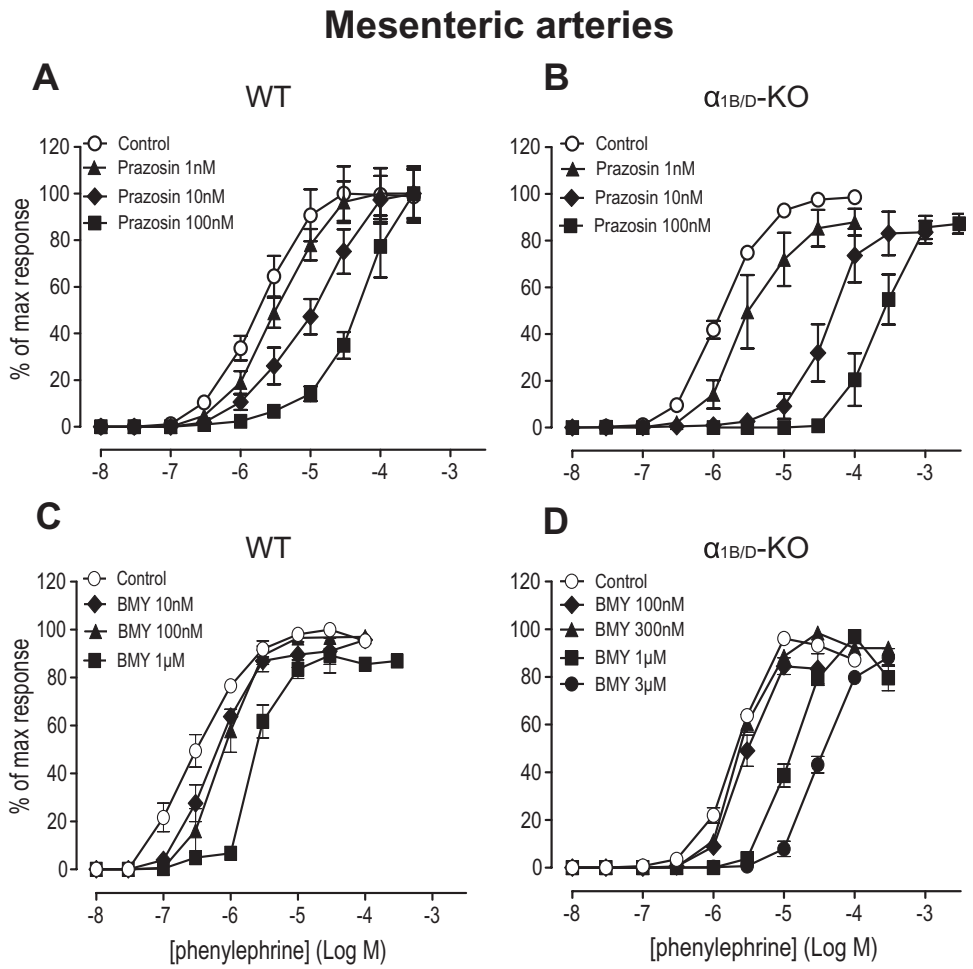

Figure 2 Effects of prazosin (A) and (B), and BMY 7378 (8-[2-[4-(2-methoxyphenyl)-1-piperazinyl]ethyl]-8-azaspiro[4.5]decane-7,9-dione) (C) and (D) on contractile response to phenylephrine in mesenteric arteries of the wild-type (WT) (n = 6) and $\alpha_{1B/D}$-adrenoceptor knockout ($\alpha_{1B/D}$-KO) mice (n = 7). Data points are expressed as percentage of control curve maximum as mean ± SEM.

Table 3 Potency values of antagonists of responses to phenylephrine and A-61603 in mouse mesenteric arteries

Antagonist	*Phenylephrine*				*A-61603*	
	WT		*$\alpha_{1B/D}$-KO*		*WT*	*$\alpha_{1B/D}$-KO*
	pA_2/pK_B	*Slope (95% CI)*	pA_2/pK_B	*Slope (95% CI)*	pK_B	pK_B
Prazosin	8.8	–	9.6	1.0 (0.8–1.2)	–	9.3
RS100-329	–	–	–	–	9.0	9.9
5-Methylurapidil	9.0	–	8.9	–	8.8	8.9
BMY 7378	8.3 (at 10 nM) 7.0 (at 1 μM)	–	6.5	1.1 (0.8–1.4)	–	6.5

A-61603, N-[5-(4,5-dihydro-1H-imidazol-2-yl)-2-hydroxy-5,6,7,8-tetrahydronaphthalen-1-yl]methanesulphonamide; $\alpha_{1B/D}$-KO, $\alpha_{1B/D}$-adrenoceptor knockout mouse; BMY 7378, 8-[2-[4-(2-methoxyphenyl)-1-piperazinyl]ethyl]-8-azaspiro[4.5]decane-7,9-dione; RS100-329, N-[(2-trifluoroethoxy)phenyl],N′-(3-thyminylpropyl) piperazine hydrochloride; WT, wild-type.

The high pA$_2$ of 9.6 calculated for the $\alpha_{1B/D}$-KO (Table 3) is consistent with α_1-adrenoceptor pharmacology at recombinant α_{1A}-adrenoceptor (Table 1). However, in the WT arteries, prazosin showed only moderate potency as indicated by the pK$_B$ of 8.8 (Table 3). Prazosin was also tested against A-61603 in the $\alpha_{1B/D}$-KO (Table 3), producing a pK$_B$ indicative of an α_1-adrenoceptor-mediated response.

The effect of the selective α_{1D}-adrenoceptor antagonist BMY 7378 was studied to examine the contractile role of the α_{1D}-adrenoceptor in the mesenteric artery. In WT arteries BMY 7378 caused parallel shifts of the phenylephrine concentration–response curve but the relationship to antagonist concentration was not clearly dose-related (Figure 2C). Thus, at the lowest BMY 7378 concentration (10 nM), the

concentration–response curve was shifted significantly to the right ($P < 0.05$). An intermediate concentration (100 nM) had little further effect but the highest concentration (1 μM) produced a further significant rightward shift ($P < 0.01$). pK_B values were calculated for BMY 7378 at the lowest and highest concentrations (Table 3), and these were comparable with α_{1D}-adrenoceptor and α_{1A}-adrenoceptor values respectively (Table 1). In the $\alpha_{1B/D}$-KO, BMY 7378, at high concentrations (300 nM, 1 μM and 3 μM), caused concentration-related, rightward shifts of the phenylephrine response curve (Figure 2D). In the tissues from this mouse strain, the pA_2 value (6.5) (Table 3) was identical to that obtained against the A-61603 response and indicates the potency of BMY 7378 at the α_{1A}-adrenoceptor.

5-Methylurapidil was employed as much of the existing literature uses this antagonist as being 'α_{1A}-adrenoceptor-selective'. In WT arteries, 5-methylurapidil caused a parallel rightward shift of the phenylephrine response at 10 nM (Figure 3A), which produced a pK_B (Table 3) indicative of an α_{1A}-adrenoceptor-mediated response (Table 1). However, 100 nM shifted only the upper part of the curve, creating a biphasic concentration–response curve, suggestive of a component of the response being attributable to either α_{1D}-adrenoceptor or α_{1B}-adrenoceptor. Consequently, 5-methylurapidil (100 nM) was studied in the α_{1B}-KO, to reduce the possibilities to the α_{1D}-adrenoceptor and α_{1A}-adrenoceptor subtypes. In this strain, 5-methylurapidil (100 nM) also revealed a biphasic response, indicating that the additional response was α_{1D}-adrenoceptor-mediated (Figure 3B). The position was further clarified by using 5-methylurapidil in combination with BMY 7378: BMY 7378 eliminated the minor component. This was quantified by showing that, while the pEC_{50} for phenylephrine in the presence of 5-methylurapidil (100 nM) was unaffected by BMY 7378 treatment (4.5 ± 0.1), the pEC_{25}, which was more representative of the first 'phase', was shifted significantly rightward by BMY 7378 from 6.4 ± 0.3 to 4.8 ± 0.1 ($P < 0.001$). The response after 5-methylurapidil plus BMY 7378 was thus monophasic (lacking the first phase) (Figure 3B). In the $\alpha_{1B/D}$-KO, a monophasic response to phenylephrine was observed in the presence of 5-methylurapidil (100 nM) (Figure 3C). The phenylephrine concentration–response curve was shifted rightward in parallel by 5-methylurapidil, producing a pK_B value (Table 3) comparable to published values for α_{1A}-adrenoceptors (Table 1).

As phenylephrine was found to be acting on more than one subtype, hence complicating assessment, antagonist potency for the α_{1A}-adrenoceptor was tested against a selective α_{1A}-adrenoceptor agonist, A-61603. Both 5-methylurapidil and a second α_{1A}-adrenoceptor antagonist, RS100-329, caused a concentration-related, parallel, rightward shift of the A-61603 response curve in both the WT and $\alpha_{1B/D}$-KO arteries (Table 3). This verifies that A-61603 activated only the α_{1A}-adrenoceptor in mesenteric arteries from both the WT and $\alpha_{1B/D}$-KO.

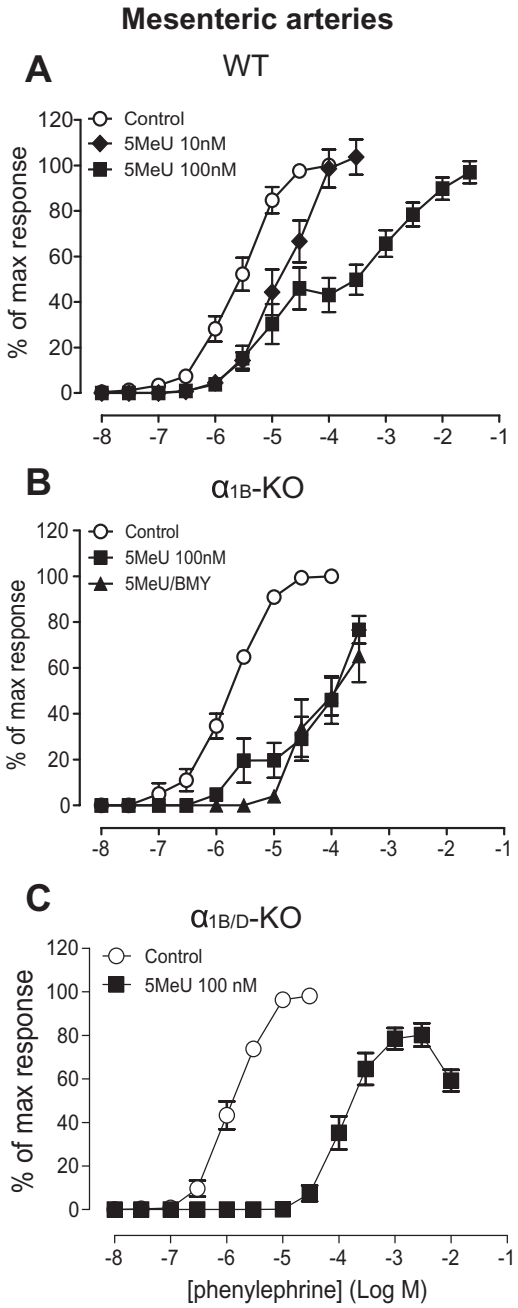

Figure 3 Effects of 5-methylurapidil (5MeU) on contractile response to phenylephrine in mouse mesenteric arteries. (A) Antagonizing effect of 5-methylurapidil in wild-type (WT) ($n = 6$). (B) Antagonizing effect of 5-methylurapidil and elimination of biphasic response by BMY 7378 (8-[2-[4-(2-methoxyphenyl)-1-piperazinyl]ethyl]-8-azaspiro[4.5]decane-7,9-dione) in α_{1B}-adrenoceptor knockout (α_{1B}-KO) ($n = 6$). (C) Elimination of biphasic response in $\alpha_{1B/D}$-KO ($n = 6$). Data points are expressed as percentage of control curve maximum as mean ± SEM.

Functional pharmacology in carotid arterial rings

In the WT and all three KO strains the maximum response and sensitivity to 5-hydroxytryptamine was similar (Table 4). This eliminates generic structural or smooth muscle sensitivity changes as a basis for differences subsequently found using drugs acting via α_1-adrenoceptors.

Concentration-dependent contractions to phenylephrine were produced in all mouse strains (Figure 4A; Table 4). Maximum response and sensitivity to phenylephrine were significantly reduced in the α_{1D}-KO compared with the WT. This suggests that the WT response can be attributed

Table 4 Agonist responses in mouse carotid arteries

Mouse	*Phenylephrine*		*A-61603*		*5-Hydroxytryptamine*	
	Maximum response (g)	p*EC*$_{50}$	*Maximum response (g)*	p*EC*$_{50}$	*Maximum response (g)*	p*EC*$_{50}$
WT	0.27 ± 0.01	6.6 ± 0.05	0.28 ± 0.02	6.0 ± 0.06	0.27 ± 0.04	6.9 ± 0.08
α_{1B}-KO	0.32 ± 0.01	6.9 ± 0.10	0.26 ± 0.02	6.3 ± 0.04*	0.27 ± 0.05	6.9 ± 0.08
α_{1D}-KO	0.17 ± 0.01***	5.6 ± 0.06***	0.14 ± 0.01***	6.7 ± 0.08***	0.26 ± 0.06	6.8 ± 0.04
$\alpha_{1B/D}$-KO	0.06 ± 0.01***	4.9 ± 0.07***	0.13 ± 0.01***	6.6 ± 0.09***	0.26 ± 0.03	6.8 ± 0.07

Maximum responses and pEC_{50} values are expressed as mean ± SEM.
A-61603, N-[5-(4,5-dihydro-1H-imidazol-2-yl)-2-hydroxy-5,6,7,8-tetrahydronaphthalen-1-yl]methanesulphonamide; α_{1B}-KO, α_{1B}-adrenoceptor knockout; α_{1D}-KO, α_{1D}-adrenoreceptor knockout; $\alpha_{1B/D}$-KO, $\alpha_{1B/D}$-adrenoceptor knockout; WT, wild-type.
*P < 0.05; ***P < 0.001 compared with WT (one-way ANOVA, Bonferroni's post test).

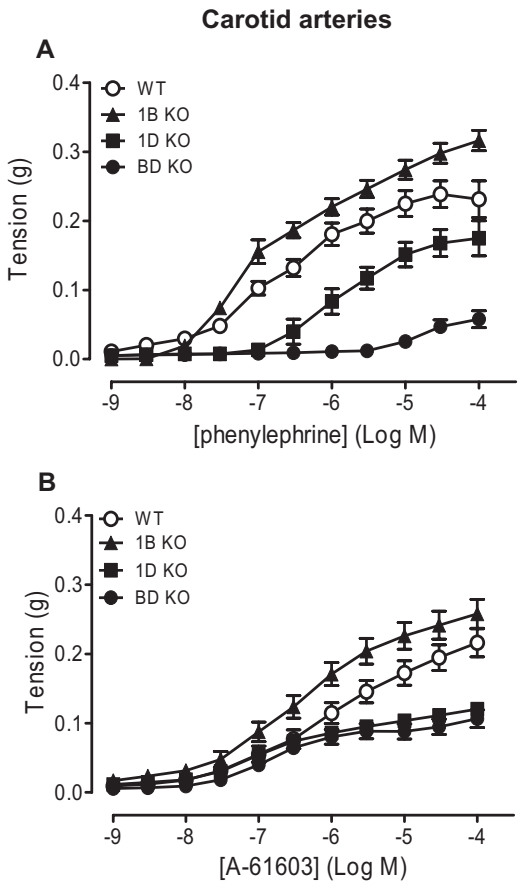

Figure 4 Contractile responses to (A) phenylephrine (n = 8) and (B) A-61603 (N-[5-(4,5-dihydro-1H-imidazol-2-yl)-2-hydroxy-5,6,7,8-tetrahydronaphthalen-1-yl]methanesulphonamide) (n = 8) in carotid arteries of wild-type (WT), α_{1B}-adrenoceptor knockout (1B KO), α_{1D}-adrenoceptor knockout (1D KO) and $\alpha_{1B/D}$-adrenoceptor knockout (BD KO) mice. Data points are expressed in g tension as mean ± SEM.

predominantly to α_{1D}-adrenoceptors and the small response in the $\alpha_{1B/D}$-KO suggests a minor contribution from α_{1A}-adrenoceptors. The effect of knocking out the α_{1B}-adrenoceptor differed according to the other receptors present. Its elimination from the WT (α_{1B}-KO) resulted in an increase in maximum response and sensitivity to phenylephrine indicating either an up-regulation of the α_{1D}- or α_{1A}-adrenoceptor-mediated response or loss of an inhibitory response. In contrast, elimination of the α_{1B}-adrenoceptors from the α_{1D}-adrenoceptor strain ($\alpha_{1B/D}$-KO) resulted in a reduction in response. This suggests the existence of an α_{1B}-adrenoceptor-mediated contraction or a down-regulation of an α_{1A}-adrenoceptor-mediated response.

The α_{1A}-adrenoceptor agonist A-61603 induced concentration-related contractions in all mouse strains (Figure 4B; Table 4). The maximum responses to A-61603 in the α_{1D}-KO and $\alpha_{1B/D}$-KO were significantly lower compared with the WT. pEC_{50} values for the A-61603-induced response were significantly higher in the α_{1B}-KO, α_{1D}-KO and $\alpha_{1B/D}$-KO than in the WT, although the pEC_{50} value to A-61603 in the α_{1B}-KO was significantly lower than in the α_{1D}-KO and $\alpha_{1B/D}$-KO ($P < 0.001$ and $P < 0.05$ respectively). This can be explained by the presence of the α_{1D}-adrenoceptors: there is an additional component at high concentrations of A-61603 that has the effect of reducing the apparent pEC_{50} value; this is eliminated after knocking out the α_{1D}-adrenoceptors, revealing the true, higher, sensitivity of A-61603 at α_{1A}-adrenoceptors. Also, for this reason, sensitivity, but not maximum response, to A-61603 appears to be significantly lower than for phenylephrine in the WT (Table 4). In the $\alpha_{1B/D}$-KO both maximum response and sensitivity to A-61603 were significantly higher than for phenylephrine, reflecting the true situation at α_{1A}-adrenoceptors, with a difference in pEC_{50} values of 1.7, similar to the value of 1.6 in the mesenteric artery.

In the carotid arteries from WT mice, prazosin competitively antagonized the phenylephrine concentration–response curve (Figure 5A; Table 5). In the $\alpha_{1B/D}$-KO the phenylephrine concentration–response curve was significantly shifted rightward by prazosin 10 nM, although a true maximum response was not achieved within the agonist concentration used (Figure 5B; Table 5).

In the WT, only 10 nM prazosin produced a parallel shift in the A-61603 curve, enabling a pK_B to be calculated (Figure 5C; Table 5). Prazosin (10 nM) also produced a parallel shift in the A-61603-induced response in the $\alpha_{1B/D}$-KO (Figure 5D) producing a pK_B (9.1), comparable to published values for α_{1A}-adrenoceptors.

In the $\alpha_{1B/D}$-KO, in the presence of the selective α_{1A}-adrenoceptor antagonist 5-methylurapidil the contractile response to phenylephrine was obliterated (Table 5). No further antagonist studies were performed against phenylephrine in the $\alpha_{1B/D}$-KO due to the low potency of the agonist in this artery.

The potency estimates for 5-methylurapidil against A-61603 were similar in the $\alpha_{1B/D}$-KO and WT (Figure S3;

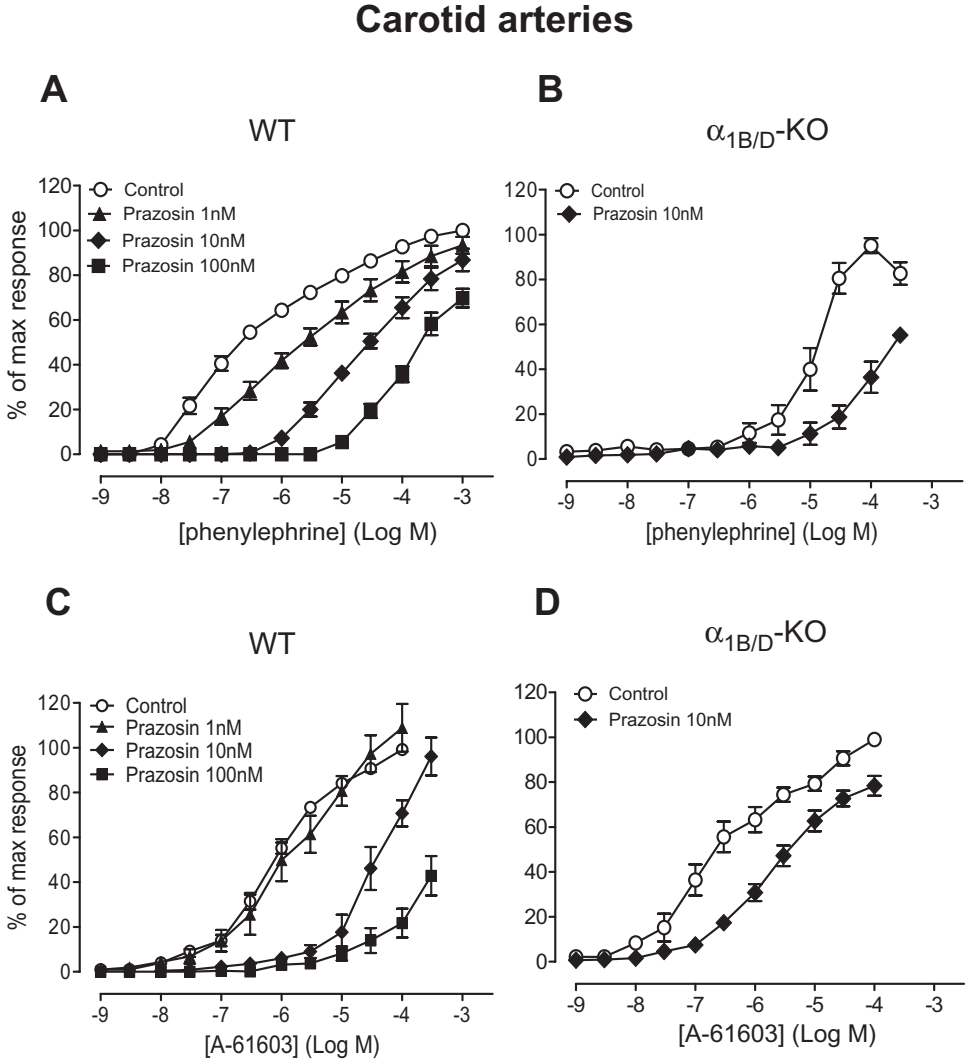

Figure 5 Effects of prazosin on contractile response to phenylephrine (A) and (B), and A-61603 (N-[5-(4,5-dihydro-1H-imidazol-2-yl)-2-hydroxy-5,6,7,8-tetrahydronaphthalen-1-yl]methanesulphonamide) (C) and (D) in carotid arteries of wild-type (WT) (n = 7) and $\alpha_{1B/D}$-adrenoceptor knockout ($\alpha_{1B/D}$-KO) (n = 6) mice. Data points are expressed as percentage of control curve maximum as mean ± SEM.

Table 5 Potency values of antagonists of responses to phenylephrine and A-61603 in mouse carotid arteries

Antagonist	*Phenylephrine*				*A-61603*			
	WT		*$\alpha_{1B/D}$-KO*		*WT*		*$\alpha_{1B/D}$-KO*	
	pA_2/pK_B	*Slope*	pA_2/pK_B	*Slope*	pA_2/pK_B	*Slope*	pA_2/pK_B	*Slope*
Prazosin	9.6*	0.9 (0.8–1.1)	9.0 at 10 nM	–	9.6 at 10 nM	–	9.1 at 10 nM	–
BMY 7378	8.3*	–	–	–	8.3	–	No shift at 10 nM and 100 nM	–
5-Methylurapidil	7.5*	1.1 (0.7–1.5)	Response abolished	–	8.3	1.0 (0.6–1.0)	8.3 at 10 nM	–
RS100-329	7.9	–	–	–	8.7	–	Non-competitive block (at 10 nM)	

A-61603, N-[5-(4,5-dihydro-1H-imidazol-2-yl)-2-hydroxy-5,6,7,8-tetrahydronaphthalen-1-yl]methanesulphonamide; $\alpha_{1B/D}$-KO, $\alpha_{1B/D}$-adrenoceptor knockout; BMY 7378, 8-[2-[4-(2-methoxyphenyl)-1-piperazinyl]ethyl]-8-azaspiro[4.5]decane-7,9-dione; RS100-329, N-[(2-trifluoroethoxy)phenyl],N′-(3-thyminylpropyl) piperazine hydrochloride; WT, wild-type.
*Denotes data from Deighan *et al.* (2005).

Table 5). Therefore, another selective α_{1A}-adrenoceptor antagonist, RS100-329, was also employed to investigate the role of the α_{1A}-adrenoceptor in the carotid artery. RS100-329 10 nM acted competitively in the WT (Figure 6A; Table 5) but blocked the A-61603-induced response in a non-competitive manner in the $\alpha_{1B/D}$-KO (Figure 6B). The pK_B for

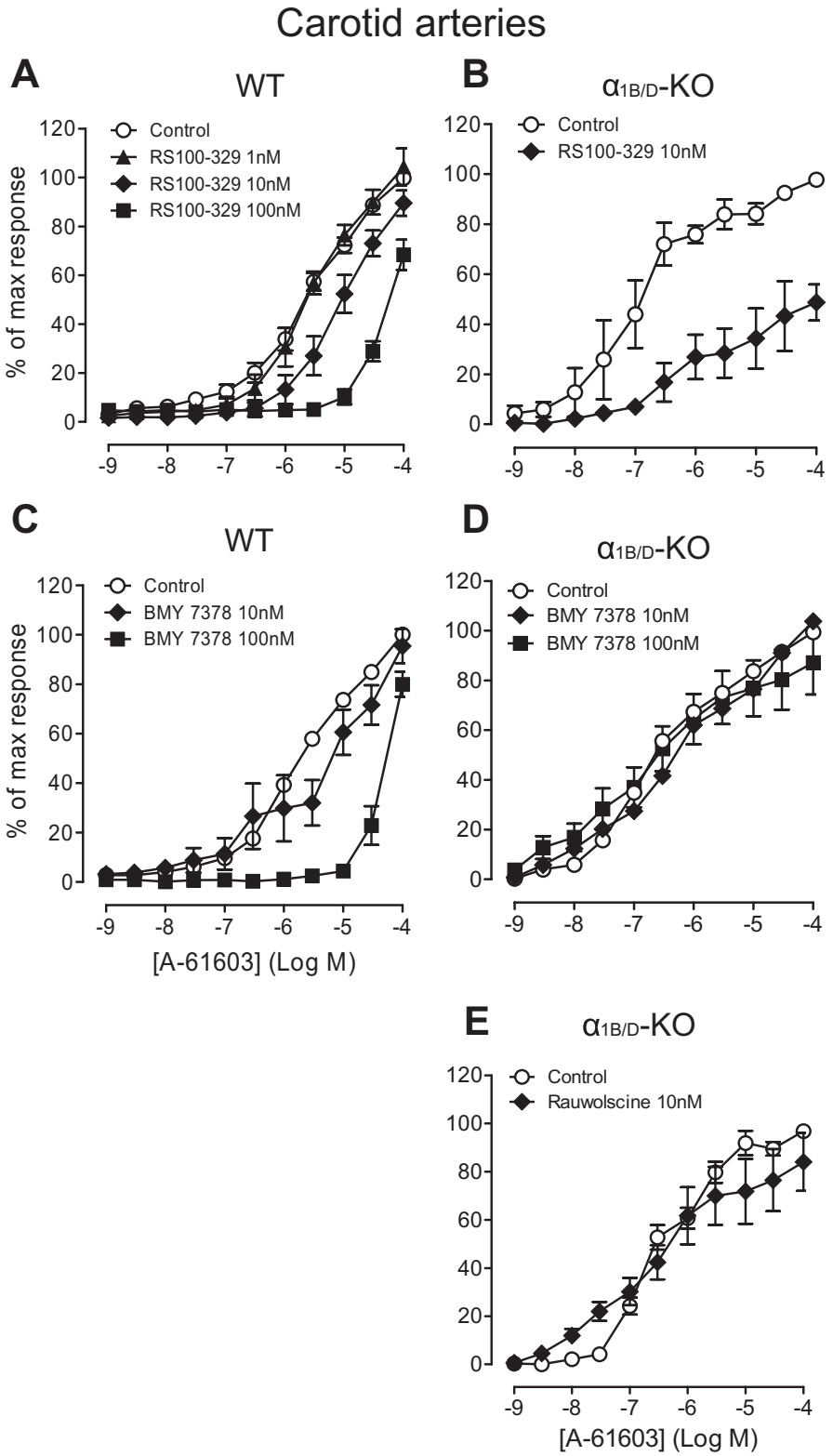

Figure 6 Effects of RS100-329 (N-[(2-trifluoroethoxy)phenyl],N′-(3-thyminylpropyl) piperazine hydrochloride) (A) and (B), BMY 7378 (8-[2-[4-(2-methoxyphenyl)-1-piperazinyl]ethyl]-8-azaspiro[4.5]decane-7,9-dione) (C) and (D), and rauwolscine (E), on contractile response to A-61603 (N-[5-(4,5-dihydro-1H-imidazol-2-yl)-2-hydroxy-5,6,7,8-tetrahydronaphthalen-1-yl]methanesulphonamide) in carotid arteries of wild-type (WT) ($n = 7$) and $\alpha_{1B/D}$-adrenoceptor knockout ($\alpha_{1B/D}$-KO) mice ($n = 7$). Data points are expressed as percentage of control curve maximum as mean ± SEM.

5-methylurapidil against A-61603 in the WT (8.3) was higher than that obtained against phenylephrine (7.5) and closer to published values for an α_{1A}-adrenoceptor-mediated response (average pK_i 8.7, Table 1).

In the WT, a biphasic response was produced in the presence of BMY 7378 10 nM (Figure 6C), highlighting the involvement of two subtypes mediating the A-61603 response, as noted above. BMY 7378 100 nM produced a rightward displacement of the A-61603 concentration–response curve producing a pK_B (Figure 6C; Table 5) in line with published values for α_{1D}-adrenoceptors (average pK_i 8.5, Table 1). This indicates α_{1D}-adrenoceptor agonism by A-61603 when an efficient α_{1D}-adrenoceptor system is present. To assess its potency versus α_{1A}-adrenoceptors and, hence, assess its selectivity, BMY 7378 was tested against A-61603 in the $\alpha_{1B/D}$-KO carotid arteries: BMY 7378 (10 nM and 100 nM) had no effect on the concentration–response curve to A-61603 (Figure 6D).

In the $\alpha_{1B/D}$-KO, the α_2-adrenoceptor antagonist, rauwolscine did not produce a rightward shift of the A-61603 concentration–response curve (Figure 6E; Table 5), suggesting that this agonist-induced response was not α_2-adrenoceptor-mediated.

Visualization of α_1-adrenoceptors using the fluorescent ligand QAPB

Mesenteric artery. In both strains, smooth muscle cells were clearly defined throughout the medial layer although the amount of fluorescence varied between individual cells (Figure 7). In the WT, QAPB appeared to bind all smooth muscle cells, while in the $\alpha_{1B/D}$-KO, some smooth muscle cells did not appear to show fluorescent ligand binding. When measured quantitatively, the intensity of fluorescence of the 96 × 96 μm image was significantly reduced in the $\alpha_{1B/D}$-KO compared with the level in the WT (Table 6). However, in the $\alpha_{1B/D}$-KO tissues, the intensity of the fluorescence of those smooth muscle cells that QAPB did bind was not significantly different to that of WT smooth muscle cells (Table 6). These data suggest that there was a reduction in the number of smooth muscle cells that bound QAPB in the $\alpha_{1B/D}$-KO mesenteric artery. Binding was present both on the cell surface and intracellularly in punctate compartments, showing that the α_{1A}-adrenoceptor is non-uniformly distributed.

Effective competition from the non-selective α_1-adrenoceptor antagonist prazosin but not from the non-selective α_2-adrenoceptor antagonist rauwolscine confirmed that the fluorescent ligand was binding to α_1-adrenoceptors and not α_2-adrenoceptors (Figure 7; Table 7).

BMY 7378 was employed at a concentration that should selectively compete with QAPB for α_{1D}-adrenoceptor binding sites in the WT and to test its ability to compete with QAPB at the α_{1A}-adrenoceptor in the $\alpha_{1B/D}$-KO. In the presence of BMY 7378 QAPB fluorescent binding was reduced in the WT but not in the $\alpha_{1B/D}$-KO (Figure 7; Table 7).

The selective α_{1A}-adrenoceptor antagonist RS100-329 was used to compete with QAPB at a concentration that should be effective at the α_{1A}-adrenoceptor but not at other potential binding sites. In the presence of RS100-329, fluorescent ligand binding was reduced in WT and abolished in $\alpha_{1B/D}$-KO (Figure 7; Table 7).

Carotid artery. Smooth muscle cells were clearly defined by QAPB binding throughout the media of the WT artery (see Figure S4) but fluorescence varied between individual cells (Figure 8). Quantitative analysis revealed that intensity of fluorescence of the 36 × 36 μm image was significantly lower in the $\alpha_{1B/D}$-KO, compared with the WT artery (Table 6). QAPB binding was more heterogeneous in the $\alpha_{1B/D}$-KO, with patches of cells virtually devoid of ligand binding. This is reflected by quantitative analysis, which showed that in smooth muscle cells showing fluorescent binding in the $\alpha_{1B/D}$-KO, the intensity of the fluorescence was not significantly different to that in the WT artery (Table 6). This suggests that the intensity of fluorescence measured for the 36 × 36 μm image reflects a reduction in the number of smooth muscle cells showing binding in the $\alpha_{1B/D}$-KO samples. In both strains, QAPB bound to both the cell surface and intracellular compartments with evidence of both perinuclear binding and punctate binding being observed intracellularly.

The use of prazosin and rauwolscine in carotid arteries confirmed that the fluorescent ligand was selective for α_1-adrenoceptors and was not binding α_2-adrenoceptors (Figure 8; Table 7).

In the WT the selective α_{1D}-adrenoceptor antagonist BMY 7378 markedly reduced QAPB binding (Figure 8; Table 7), demonstrating that the α_{1D}-adrenoceptor is present in the WT. In the $\alpha_{1B/D}$-KO, the lack of effect of BMY 7378 on fluorescence showed that BMY 7378 did not compete with QAPB for α_{1A}-adrenoceptor binding sites (Figure 8; Table 7).

Using the selective α_{1A}-adrenoceptor antagonist, RS100-329, to compete with QAPB showed reduced binding in the WT indicating that the α_{1A}-adrenoceptor is present in this strain (Figure 8; Table 7). In the $\alpha_{1B/D}$-KO, QAPB binding was quantitatively reduced and could not be detected by visual inspection in the presence of RS100-329 (Figure 8; Table 7).

Discussion

The $\alpha_{1B/D}$-KO strain shows 'pure' α_{1A}-adrenoceptor pharmacology and elucidates the complex pharmacology of the WT. Potencies of agonists and antagonists in the WT did not correlate with any single subtype as shown in pure assay systems. By working back from the $\alpha_{1B/D}$-KO, the subtypes in the WT tissues could be identified. α_{1A}-adrenoceptor-mediated contraction was identified in both arteries but was greater in the mesenteric artery. Both arteries showed α_{1D}-adrenoceptor-mediated contraction but this was greater in the carotid. There was indirect evidence for contraction by α_{1B}-adrenoceptors only in the carotid, but, in both arteries, removal of α_{1B}-adrenoceptors from the WT enhanced α_{1D}- or α_{1A}-adrenoceptor-mediated contractions.

The tissues from the $\alpha_{1B/D}$-KO provide the first genuine example of α_{1A}-adrenoceptor pharmacology in native tissues. In particular, the $\alpha_{1B/D}$-KO mesenteric artery represents a more accurate assay for functional pharmacology of the α_{1A}-adrenoceptor than is otherwise available and can be used to interpret data from other species in which KO are impractical.

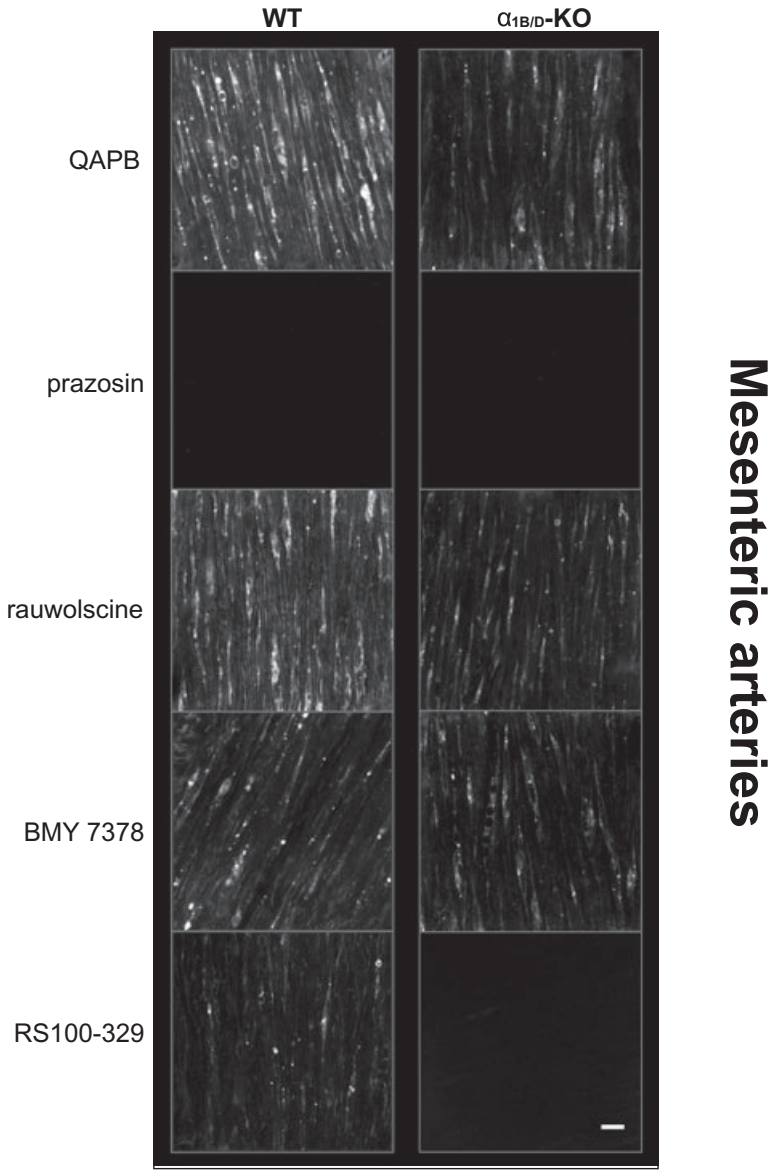

Figure 7 Comparison of QAPB fluorescent ligand binding in mesenteric arteries of WT and $\alpha_{1B/D}$-KO mice. Non-fluorescent antagonists (100 nM) were used to compete with the fluorescent ligand QAPB (100 nM) after QAPB equilibrium was established. All images are collected under identical conditions of laser intensity, photomultiplier gain (contrast) and offset (brightness). Imaging was performed at low power (zoom 3). An image size of 512 × 512 pixels produced a field size of 96 × 96 μm. Calibration bar indicates 10 μm. Each image is representative of those generated from four mice. $\alpha_{1B/D}$-KO, $\alpha_{1B/D}$-adrenoceptor knockout mouse; BMY 7378, 8-[2-[4-(2-methoxyphenyl)-1-piperazinyl]ethyl]-8-azaspiro[4.5]decane-7,9-dione; QAPB, BODIPY FL-Prazosin; RS100-329, N-[(2-trifluoroethoxy)phenyl],N′-(3-thyminylpropyl) piperazine hydrochloride; WT, wild-type.

Deviations from radioligand binding estimates are now shown to be consistent with 'contamination' of the assay vessels with other α_1-adrenoceptor subtypes. Similarly, supposed 'species' or 'tissue-specific' differences may be due to varying proportions of different subtypes.

The only evidence for genetic compensation was enhancement of α_{1A}-adrenoceptor-mediated contraction in the mesenteric artery: the maximum response of A-61603 increased when moving from the WT to $\alpha_{1B/D}$-KO. This must mean some increase in the efficiency of α_{1A}-adrenoceptors, whether by up-regulation of receptor number or signalling system. This would have been missed by studying only phenylephrine, because loss of its potent α_{1D}-adrenoceptor response negates the gain in α_{1A}-adrenoceptor response. Imaging data did not provide evidence for an up-regulation of α_{1A}-adrenoceptors in the $\alpha_{1B/D}$-KO mesenteric artery. This suggests that 'compensation' lies in the signalling process. This is specific to the α_{1A}-adrenoceptor as the 5-hydroxytryptamine response was unaffected by the loss of the α_{1B}- and α_{1D}-adrenoceptors.

Pharmacology of α_{1A}-adrenoceptors

In the $\alpha_{1B/D}$-KO, pharmacological analysis provided a clear profile for the α_{1A}-adrenoceptor. In both arteries, A-61603 had greater efficacy and potency than phenylephrine: the potency ratio was similar (40-fold). This differential is less than that

Table 6 Comparison of average pixel intensity of entire image and smooth muscle cells (SMC) in wild-type (WT) and $\alpha_{1B/D}$-adrenoceptor knockout mouse ($\alpha_{1B/D}$-KO)

Mouse strain	*Mesenteric arteries*		*Carotid arteries*	
	Average pixel intensity of 96 × 96 μm image	*Average pixel intensity of SMC*	*Average pixel intensity 36 × 36 μm image*	*Average pixel intensity of SMC*
WT	79.9 ± 4.1	84.8 ± 2.6	41.2 ± 9.2	48.8 ± 2.5
$\alpha_{1B/D}$-KO	24.3 ± 2.3***	75.7 ± 3.7	20.6 ± 2.9*	50.4 ± 3.6

Data are expressed as mean ± SEM.
Mesenteric arteries imaged at low power (zoom 3); carotid arteries imaged at high power (zoom 8).
Only smooth muscle cells showing fluorescent ligand binding were outlined as a Region of Interest to measure average pixel intensity.
$P > 0.05$ for smooth muscle cells, $\alpha_{1B/D}$-KO compared with WT (Student's *t*-test).
*$P < 0.05$; ***$P < 0.001$ compared with WT (Student's *t*-test).

Table 7 Effect of subtype-selective antagonists on fluorescent ligand binding in mesenteric and carotid arteries

Antagonist	*Average pixel intensity*			
	WT		*$\alpha_{1B/D}$-KO*	
	Mesenteric arteries	*Carotid arteries*	*Mesenteric arteries*	*Carotid arteries*
QAPB control	79.9 ± 4.1	41.2 ± 9.2	24.3 ± 2.3	20.6 ± 2.9
Prazosin	13.3 ± 7.7***	5.9 ± 1.4***	7.4 ± 1.2***	4.7 ± 1.9**
Rauwolscine	74.4 ± 10.7	55.3 ± 9.3	23.1 ± 1.3	17.3 ± 2.8
BMY 7378	27.7 ± 3.1***	10.0 ± 0.6**	24.6 ± 1.9	16.8 ± 2.6
RS100-329	24.4 ± 1.2***	13.3 ± 2.9**	9.1 ± 1.3***	5.5 ± 0.6***

Data are expressed as mean ± SEM; mesenteric arteries imaged at low power; carotid arteries imaged at high power (zoom 8).
$\alpha_{1B/D}$-KO, $\alpha_{1B/D}$-adrenoceptor knockout; BMY 7378, 8-[2-[4-(2-methoxyphenyl)-1-piperazinyl]ethyl]-8-azaspiro[4.5]decane-7,9-dione; QAPB, BODIPY FL-Prazosin; RS100-329, N-[(2-trifluoroethoxy)phenyl],N′-(3-thyminylpropyl) piperazine hydrochloride; WT, wild-type.
**$P < 0.01$; ***$P < 0.001$ compared with QAPB control (one-way ANOVA, Bonferroni's post test).

reported by Pediani *et al*. (2000) for recombinant bovine α_{1A}-adrenoceptors (70-fold) or for WT tissues by Knepper *et al*. (1995) (rat vas deferens, 300-fold; canine prostate, 165-fold) but was closer to radioligand binding at bovine α_{1A}-adrenoceptors [60-fold; (Pediani *et al*., 2000)]. Both agonists had lower potency in the carotid (approximately 50-fold) indicating a smaller receptor reserve for α_{1A}-adrenoceptors.

In the carotid, the data from A-61603 clarify the phenylephrine data. Because responses to A-61603 are similar in the α_{1D}-KO and $\alpha_{1B/D}$-KO this confirms that the reduction in the phenylephrine response is caused by the loss of an α_{1B}-adrenoceptor-mediated contraction to phenylephrine, which A-61603 does not activate. Conversely, the similarity of the increases in response to A-61603 and phenylephrine in the α_{1B}-KO suggests that this change is not due to the loss of an inhibitory effect of the agonists via α_{1B}-adrenoceptors (as A-61603 is not a good agonist at α_{1B}-adrenoceptors) but rather is a compensatory effect on the signalling process or receptor number for α_{1D}- or α_{1A}-adrenoceptors.

The functional pharmacology was straightforward in mesenteric arteries where α_{1A}-adrenoceptor is dominant in the WT strain; the major gain in accuracy was for the α_{1D}-adrenoceptor antagonist BMY 7378, whose estimated affinity fell to its α_{1A}-adrenoceptor value in the $\alpha_{1B/D}$-KO. In contrast, the selective α_{1A}-adrenoceptor antagonists, RS100-329 and 5-methylurapidil, retained high potency, as expected in the $\alpha_{1B/D}$-KO mice. A complication in the analysis of the $\alpha_{1B/D}$-KO mesenteric arteries was that prazosin was less potent in the WT than in the $\alpha_{1B/D}$-KO tissues. This was unexpected and, although this cannot be fully explained as yet, it reflects the complexity of analysis in the WT. It is interesting that the 'α_{1L}-adrenoceptor' phenomenon, that is, low affinity for prazosin (Flavahan and Vanhoutte, 1986; Muramatsu *et al*., 1990) has been reported to be lost in the α_{1A}-KO (Muramatsu *et al*., 2008), yet isolation of the α_{1A}-adrenoceptor (in the present study) does not reveal it. Thus the 'α_{1L}-adrenoceptor' phenomenon may require the presence of both the α_{1A}-adrenoceptor and another subtype.

In carotid arteries, where the residual α_{1A}-adrenoceptor response to agonists is small, the response was not sufficiently robust to sustain a comprehensive analysis. Threshold sensitivities to antagonists were as expected but were difficult to quantify in competitive terms. In addition, RS100-329 produced non-competitive blockade. Non-competitive blockade of recombinant α_{1A}-adrenoceptors has been shown for prazosin and WB4101 and was attributed to the non-equilibrium nature of post-receptor events (Pediani *et al*., 2000). Similar factors may apply here, where the maximum response achievable is small, relative to the capability of the artery, as shown by 5-hydroxytryptamine.

Agonist activity at α_{1D}-adrenoceptors by A-61603 was revealed in the KO. In the carotid, this occurred at high agonist concentrations as introducing the α_{1D}-KO reduced the responses to A-61603. Furthermore, the A-61603-induced response has an α_{1D}-adrenoceptor component in the WT, as there was a biphasic response to A-61603 in the presence of

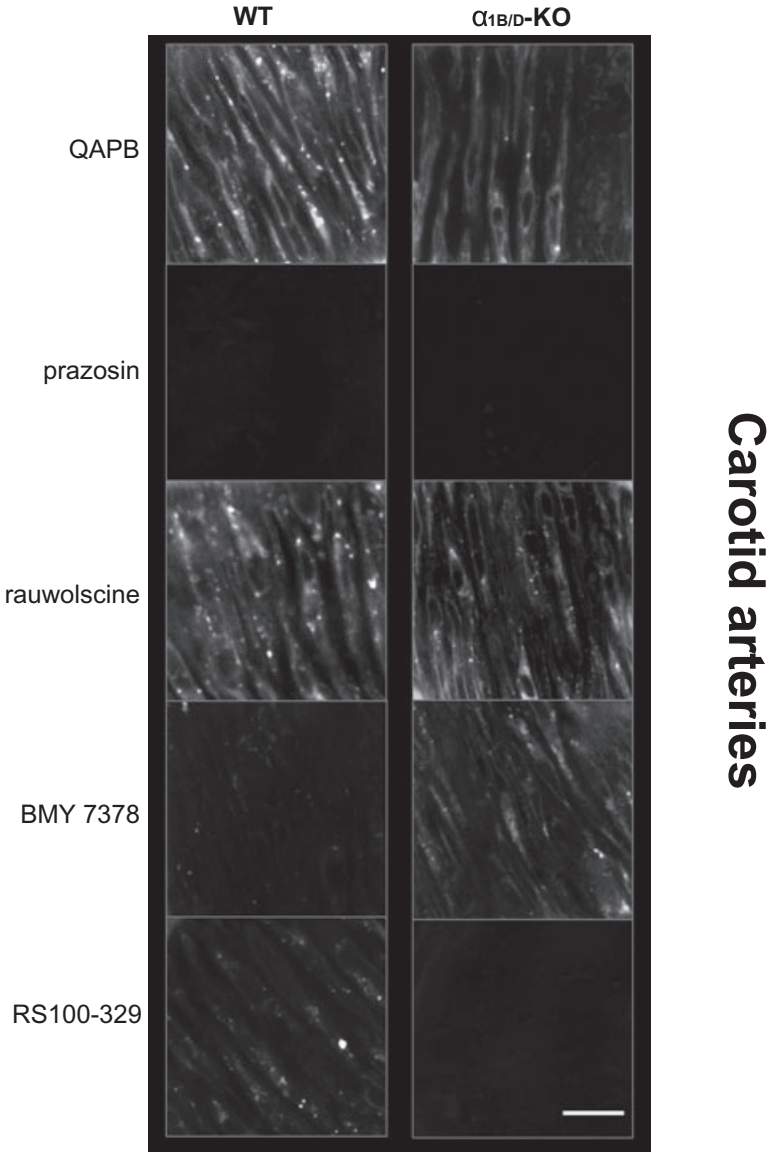

Figure 8 Comparison of QAPB fluorescent ligand binding in carotid arteries of WT and $\alpha_{1B/D}$-KO mice. Non-fluorescent antagonists (100 nM) were used to compete with QAPB (100 nM) after QAPB equilibrium was established. All images are collected under identical conditions of laser intensity, photomultiplier gain (contrast) and offset (brightness). Imaging was performed at high power (zoom 8) to include only smooth muscle cell and avoid elastic lamina in the media. An image size of 512 × 512 pixels produced a field size of 36 × 36 μm. Calibration bar indicates 10 μm. Each image is representative of those generated from four mice. $\alpha_{1B/D}$-KO, $\alpha_{1B/D}$-adrenoceptor knockout; BMY 7378, 8-[2-[4-(2-methoxyphenyl)-1-piperazinyl]ethyl]-8-azaspiro[4.5]decane-7,9-dione; QAPB, BODIPY FL-Prazosin; RS100-329, N-[(2-trifluoroethoxy)phenyl],N′-(3-thyminylpropyl) piperazine hydrochloride; WT, wild-type.

BMY 7378 10 nM and the potency estimate for BMY 7378 (100 nM) was comparable to the α_{1D}-adrenoceptor values (Table 1). This did not occur in the mesenteric artery where the receptor reserve for α_{1D}-adrenoceptor is smaller, consistent with A-61603 being a partial agonist at α_{1D}-adrenoceptor. This detailed pharmacological information refines the ability to assess the presence of the subtypes in non-genetically modified species.

Location of α_{1A}-adrenoceptors

When α_{1A}-adrenoceptors were isolated in the $\alpha_{1B/D}$-KO they showed, in general, a more heterogeneous distribution than when the whole family of subtypes was present in the WT. This was most apparent in the carotid, where the α_{1A}-adrenoceptor is secondary to the α_{1D}-adrenoceptor. This suggests a general phenomenon of different phenotypes of vascular smooth muscle in respect of α_{1A}-adrenoceptors. This may be relevant to function, for example, of pacemaker cells (Peng *et al*., 2001) and partly explains the reduced maximum response in the $\alpha_{1B/D}$-KO carotid, in which there is less likely to be a functional syncytium due to the separation of smooth muscle cells by collagen layers: consequently, the maximum response becomes dependent on the number of cells expressing the receptors, in contrast to a functional syncytium such as in the mesenteric artery where depolarization can spread

through the tissue despite a limited number of cells expressing receptors.

In both arteries, receptors were found both on the cell surface and in intracellular compartments, reflecting findings in cell cultures with recombinant α_{1D}- (Daly *et al*., 1998) and α_{1A}-adrenoceptors (Pediani *et al*., 2005). This seems to be a genuine phenotype and not an artefact. Vascular fibroblasts in intact arteries also have a substantial population of intracellular α_1-adrenoceptors (McGrath *et al*., 2005), so the phenomenon is a general one for native and recombinant α_1-adrenoceptors, expressed in different cell types. In addition, fixed and permeabilized tissues also show these different cellular phenotypes (Miquel *et al*., 2005) eliminating differential ligand uptake as an explanation. There is no simple explanation based on different proportions of the subtypes in these different phenotypes or chaperoning by heterodimers. Nevertheless, increased heterogeneity in both types of artery, once the other subtypes were eliminated, shows a strong tendency for the α_{1A}-adrenoceptor subtype to be heterogeneously distributed.

Potential interaction of α_1-adrenoceptor subtypes

This is the first example of a native tissue in which it has been possible to observe the consequences, for receptor distribution, of moving from the WT strain with multiple subtypes of α_1-adrenoceptor to a double KO expressing only one subtype. There was, however, no evidence that removing the α_{1B}-adrenoceptor had any influence on the balance of surface to intracellular distribution of the remaining subtypes, as had been inferred from artificial systems (Stanasila *et al*., 2003; Hague *et al*., 2004b).

Physiological and therapeutic relevance

Our demonstration of the likely presence of all three subtypes in native vascular smooth muscle cells is extremely interesting for physiological function. The relative preponderance of the subtypes, as shown by fluorescent ligand binding, was similar between the two arteries despite the quantitatively different contribution of the subtypes to contraction. Thus, measuring the presence of the receptor or its RNA will not give a useful guide to function and, perhaps, the relative contribution of each subtype is more effectively regulated by other factors than by the amount of receptor present. This correlates also with functional compensation of the α_{1A}-adrenoceptor for the loss of the other two subtypes, which showed as an increase in response without evidence for an up-regulation of the receptors present.

As binding and function both show multiple subtypes in these two arteries, it is not beneficial to assign one α_1-adrenoceptor subtype to a specific vessel or to a class of vessel that performs a particular physiological function. α_1-Adrenoceptor heterogeneity is an important consideration when assessing the selectivity of α_1-adrenoceptor compounds. Blockade of either α_{1A}-adrenoceptor or α_{1D}-adrenoceptor can affect the response and, thus, can be expected to block adrenergic control of peripheral resistance, as has been demonstrated *in vivo* (Villalobos-Molina and Ibarra, 1996; Zhou and Vargas, 1996) and *in vitro* (Castillo *et al*., 1998; Zacharia *et al*., 2004; 2005). This indicates that no one subtype plays a part in maintaining and regulating blood pressure as suggested by the mild hypotension in each single KO model (Rokosh and Simpson, 2002; Tanoue *et al*., 2002a).

Acknowledgements

This paper is dedicated to the memory of the late Ann McGee, preliminary studies carried out by Ann provided the impetus for this work. The authors thank Mrs Joyce Macmillan for her expert technical assistance. M McBride and L Methven received generous support from the British Heart Foundation (PG/05/140/20094 and FS/04/035) and the Ann B McNaught Bequest.

Conflict of interest

None.

References

Alexander SPH, Mathie A, Peters JA (2008). Guide to Receptors and Channels (GRAC). *Br J Pharmacol* **153**: S14.

Buckner SA, Oheim KW, Morse PA, Knepper SM, Hancock AA (1996). Adrenoceptor-induced contractility in rat aorta is mediated by the alpha (1D) subtype. *Eur J Pharmacol* **297**: 241–248.

Castillo EF, López RM, Rodríguez-Silverio J, Bobadilla RA, Castillo C (1998). Alpha 1D-adrenoceptors contribute to the neurogenic vasopressor response in pithed rats. *Fundam Clin Pharmacol* **12**: 584–589.

Cavalli A, Lattion AL, Hummler E, Nenniger M, Pedrazzini T, Aubert JF *et al*. (1997). Decreased blood pressure response in mice deficient of the alpha 1b-adrenergicreceptor. *Proc Natl Acad Sci* **94**: 11589–11594.

Daly CJ, McGrath I (2003). Fluorescent ligands, antibodies, and proteins for the study of receptors. *Pharmacol Ther* **100**: 101–118.

Daly CJ, Milligan CM, Milligan G, Mackenzie JF, McGrath JC (1998). Cellular localization and pharmacological characterization of functioning alpha-1 adrenoceptors by fluorescent ligand binding and image analysis reveals identical binding properties of clustered and diffuse populations. of receptors. *J Pharmacol Exp Ther* **286**: 984–990.

Daly CJ, Deighan C, McGee A, Mennie D, Ali Z, McBride M *et al*. (2002). A knockout approach indicates a minor vasoconstrictor role for vascular α_{1B}-adrenoceptors in mouse. *Physiol Genomics* **9**: 85–91.

Deighan C, Woollhead A, Colston J, McGrath JC (2004). Hepatocytes from α_{1B}-adrenoceptor knockout mice reveal compensatory adrenoceptor subtype substitution. *Br J Pharmacol* **142**: 1031–1037.

Deighan C, Methven L, Naghadeh MM, Wokoma A, MacMillan J, Daly CJ *et al*. (2005). Insights into the functional roles of α_1-adrenoceptor subtypes in mouse carotid arteries using knockout mice. *Br J Pharmacol* **144**: 558–565.

Flavahan NA, Vanhoutte PM (1986). [alpha]1-adrenoceptor subclassification in vascular smooth muscle. *Trends Pharmacol Sci* **7**: 347–349.

Garcia-Sainz JA, Romero-Avila M, Torres-Marquez ME (1995). Characterization of the human liver alpha 1-adrenoceptors: predominance of the alpha 1A subtype. *Eur J Pharmacol* **289**: 81–86.

Goetz AS, Lutz MW, Rimele TJ, Saussy DLJ (1994). Characterisation of alpha-1-adrenoceptor subtypes in human and canine prostate membrane. *J Pharmacol Exp Ther* **271**: 1228–1233.

Goetz AS, King HK, Ward SDC, True TA, Rimele TJ, Saussy J (1995).

BMY 7378 is a selective antagonist of the D subtype of [alpha]1-adrenoceptors. *Eur J Pharmacol* **272**: R5–R6.

Gross G, Hanft G, Rugevics C (1988). 5-Methyl-urapidil discriminates between subtypes of the [alpha]1-adrenoceptor. *Eur J Pharmacol* **151**: 333–335.

Guimaraes S, Moura D (2001). Vascular adrenoceptors: an update. *Pharmacol Rev* **53**: 319–356.

Hague C, Chen Z, Pupo AS, Schulte NA, Toews ML, Minneman KP (2004a). The N terminus of the human alpha1D-adrenergic receptor prevents cell surface expression. *J Pharmacol Exp Ther* **309**: 388–397.

Hague C, Uberti M, Chen Z, Hall R, Minneman KP (2004b). Cell surface expressin of alpha 1D-adrenergic receptors is controlled by heterodimerization with alpha 1B-adrenergic receptors. *J Biol Chem* **279** (15): 15541–15549.

Hieble JP, Bylund DB, Clarke DE, Eikenburg DC, Langer SZ, Lefkowitz RJ *et al.* (1995). International Union of Pharmacology. X. Recommendation for nomenclature of alpha 1-adrenoceptors: consensus update. *Pharmacol Rev* **47**: 267–270.

Hirasawa A, Sugawara T, Awaji T, Tsumaya K, Ito H, Tsujimoto G (1997). Subtype-specific differences in subcellular localization of alpha 1-adrenoceptors: chlorethylclonidine preferentially alkylates the accessible cell surface alpha 1-adrenoceptors irrespective of the subtype. *Mol Pharmacol* **52**: 764–770.

Hosoda C, Koshimizu TA, Tanoue A, Nasa Y, Oikawa R, Tomabechi T *et al.* (2005). Two alpha1-adrenergic receptor subtypes regulating the vasopressor response have differential roles in blood pressure regulation. *Mol Pharmacol* **67**: 912–922.

Hrometz SL, Edelmann SE, McCune DF, Olges JR, Hadley RW, Perez DM *et al.* (1999). Expression of multiple alpha 1-adrenoceptors on vascular smooth muscle: correlation with the regulation of Contraction. *J Pharmacol Exp Ther* **290**: 452–463.

Kenny BA, Chalmers DH, Philpott PC, Naylor AM (1995). Characterization of an α_{1D}-adrenoceptor mediating the contractile response of rat aorta to noradrenaline. *Br J Pharmacol* **115**: 981–986.

Knepper SM, Buckner SA, Brune ME, DeBernardis JF, Meyer MD, Hancock AA (1995). A-61603, a potent alpha 1-adrenergic receptor agonist, selective for the alpha 1A receptor subtype. *J Pharmacol Exp Ther* **274**: 97–103.

Leonardi A, Heible JP, Guarneri L, Naselsky DP, Poggesi E, Sironi G *et al.* (1997). Pharmacological characterization of the uroselective alpha-1 antagonist Rec 15/2739 (SB 216469): role of the alpha-1L adrenoceptor in tissue selectivity, part I. *J Pharmacol Exp Ther* **281**: 1272–1283.

McCune DF, Edelmann SE, Olges JR, Post GR, Waldrop BA, Waugh DJJ *et al.* (2000). Regulation of the cellular localization and signaling properties of the alpha 1B- and alpha 1D-adrenoceptors by agonists and inverse agonists. *Mol Pharmacol* **57**: 659–666.

McGrath I, Deighan C, Briones A, Malekzadeh-Shafaroudi M, McBride M, Adler J *et al.* (2005). New aspects of vascular remodelling: the involvement of all vascular cell types. *Exp Physiol* **90**: 469–475.

Mackenzie JF, Daly CJ, Pediani JD, McGrath JC (2000). Quantitative imaging in live human cells reveals intracellular alpha 1-adrenoceptor ligand-binding sites. *J Pharmacol Exp Ther* **294**: 434–443.

Martinez-Salas SG, Campos-Peralta JM, Pares-Hipolito J, Gallardo-Ortiz IA, Ibarra M, Villalobos-Molina R (2007). Alpha-1A adrenoceptors predominate in the control of blood pressure in mouse mesenteric vascular bed. *Auton Autacoid Pharmacol* **27**: 137–142.

Meyer MD, Altenbach RJ, Hancock AA, Buckner SA, Knepper SM, Kerwin JF (1996). Synthesis and in vitro characterization of N-[5-(4,5-dihydro-1H-imidazol-2-yl)-2-hydroxy-5,6,7,8-tetrahydronaphthalen-1-yl]methanesulfonamide and its enantiomers: a novel selective alpha-1a receptor agonist. *J Med Chem* **39**: 4116–4119.

Michel MC, Goepel M (1998). Differential alpha-1 adrenoceptor labeling by [3H]-prazosin and [3H]-tamsulosin. *Eur J Pharmacol* **342**: 85–92.

Miquel RM, Segura V, Ali Z, D'Ocon P, McGrath JC, Daly CJ (2005). 3-D image analysis of fluorescent drug binding. *Mol Imaging* **4**: 1–13.

Morris DP, Price RR, Smith MP, Lei B, Schwinn DA (2004). Cellular trafficking of human {alpha}1a-adrenergic receptors is continuous and primarily agonist-independent. *Mol Pharmacol* **66**: 843–854.

Muramatsu I, Ohmura T, Kigoshi S, Hashimoto S, Oshita M (1990). Pharmacological subclassification of α_1-adrenoceptors in vascular smooth muscle. *Br J Pharmacol* **99**: 197–201.

Muramatsu I, Morishima S, Suzuki F, Yoshiki H, Anisuzzaman ASM, Tanaka T *et al.* (2008). Idenitifcation of α_{1L}-adrenoceptor in mice and its abolition by α_{1A}-adrenoceptor gene knockout. *Br J Pharmacol* **155**: 1224–1234.

Pediani J, Mackenzie JF, Heeley RP, Daly CJ, McGrath JC (2000). Single-cell recombinant pharmacology: bovine alpha-1a adrenoceptors in rat-1 fibroblasts release intracellular calcium, display subtype-characteristic agonism and antagonism and exhibit an antagonist-reversible inverse concentration-response phase. *J Pharmacol Exp Ther* **293**: 895.

Pediani JD, Colston JF, Caldwell D, Milligan G, Daly CJ, McGrath JC (2005). Beta-arrestin-dependent spontaneous alpha-1a-adrenoceptor endocytosis causes intracellular transportation of alpha-blockers via recycling compartments. *Mol Pharmacol* **67**: 1004.

Peng H, Matchkov V, Ivarsen A, Aalkjar C, Nilsson H (2001). Hypothesis for the initiation of vasomotion. *Circ Res* **88**: 810–815.

Piascik MT, Hrometz SL, Edelmann SE, Guarino RD, Hadley RW, Brown RD (1997). Immunocytochemical localization of the alpha-1B adrenergic receptor and the contribution of this and the other subtypes to vascular smooth muscle contraction: analysis with selective ligands and antisense oligonucleotides. *J Pharmacol Exp Ther* **283**: 854–868.

Rokosh DG, Simpson PC (2002). Knockout of the alpha 1A/C-adrenergic receptor subtype: the alpha 1A/C is expressed in resistance arteries and is required to maintain arterial blood pressure. *Proc Natl Acad Sci* **99**: 9474–9479.

Saussy DJ, Goetz AS, Queen KL, King HK, Lutz MW, Rimele TJ (1996). Structure activity relationships of a series of buspirone analogs at alpha-1 adrenoceptors: further evidence that rat aorta alpha-1 adrenoceptors are of the alpha-1D-subtype. *J Pharmacol Exp Ther* **278**: 136–144.

Stanasila L, Perez JB, Vogel H, Cotecchia S (2003). Oligomerization of the {alpha}1a- and {alpha}1b-adrenergic receptor subtypes: potential implications in receptor internalization. *J Biol Chem* **278**: 40239–40251.

Sugawara T, Hirasawa A, Hashimoto K, Tsujimoto G (2002). Differences in the subcellular localization of α1-adrenoceptor subtypes can affect the subtype selectivity of drugs in a study with the fluorescent ligand BODIPY FL-prazosin. *Life Sci* **70**: 2113–2124.

Tanoue A, Koba M, Miyawaki S, Koshimizu TA, Hosoda C, Oshikawa S *et al.* (2002a). Role of the {alpha}1D-adrenegric receptor in the development of salt-induced hypertension. *Hypertension* **40**: 101–106.

Tanoue A, Nasa Y, Koshimizu T, Shinoura H, Oshikawa S, Kawai T *et al.* (2002b). The {alpha}1D-adrenergic receptor directly regulates arterial blood pressure via vasoconstriction. *J Clin Invest* **109**: 765–775.

Testa R, Guarneri L, Angelico P, Poggesi E, Taddei C, Sironi G *et al.* (1997). Pharmacological characterization of the uroselective alpha-1 antagonist Rec 15/2739 (SB 216469): role of the alpha-1L adrenoceptor in tissue selectivity, part II. *J Pharmacol Exp Ther* **281**: 1284–1293.

Turnbull L, McCloskey DT, O'Connell TD, Simpson PC, Baker AJ (2003). Alpha 1-adrenergic receptor responses in alpha 1AB-AR knockout mouse hearts suggest the presence of alpha 1D-AR. *Am J Physiol Heart Circ Physiol* **284**: H1104–H1109.

Uberti M, Hall R, Minneman KP (2003). Subtype-specific dimerization of alpha1-adrenoceptors: effects on receptor expression and pharmacological properties. *Mol Pharmacol* **64**: 1379–1390.

Villalobos-Molina R, Ibarra M (1996). [alpha]1-Adrenoceptors mediating contraction in arteries of normotensive and spontaneously hypertensive rats are of the [alpha]1D or [alpha]1A subtypes. *Eur J Pharmacol* **298**: 257–263.

Williams TJ, Blue DR, Daniels DV, Davis B, Elworthy T, Gever JR *et al*. (1999). In vitro α1-adrenoceptor pharmacology of Ro 70-0004 and RS-100329, novel α_{1A}-adrenoceptor selective antagonists. *Br J Pharmacol* **127**: 252–258.

Yoshio R, Taniguchi T, Itoh H, Muramatsu I (2001). Affinity of serotonin receptor antagonists and agonists to recombinant and native alpha1-adrenoceptor subtypes. *Jpn J Pharmacol* **86**: 189–195.

Zacharia J, Hillier C, MacDonald A (2004). α_1-Adrenoceptor subtypes involved in vasoconstrictor responses to exogenous and neurally released noradrenaline in rat femoral resistance arteries. *Br J Pharmacol* **141**: 915–924.

Zacharia J, Hillier C, Tanoue A, Tsujimoto G, Daly CJ, McGrath JC *et al*. (2005). Evidence for involvement of α_{1D}-adrenoceptors in contraction of femoral resistance arteries using knockout mice. *Br J Pharmacol* **146**: 942–951.

Zhou l, Vargas HM (1996). Vascular alpha 1D-adrenoceptors have a role in the pressor response to phenylephrine in the pithed rat. *Eur J Pharmacol* **305**: 173–176.

Supporting information

Additional Supporting Information may be found in the online version of this article:

Figure S1 Example of abolishment of BODIPY FL-Prazosin (QAPB) binding by prazosin (left image) but presence of smooth muscle cells confirmed by the nuclear stain Syto 61 (right image) in carotid artery of wild-type (WT). Imaging was performed at high power (zoom 8) to include only smooth muscle cells and avoid elastic lamina in the media. An image size of 512 × 512 pixels produced a field size of 36 μm × 36 μm. Calibration bar indicates 5 μm.

Figure S2 Illustration of measurement of average pixel intensity from individual smooth muscle cells from wild-type (WT) and $\alpha_{1B/D}$-adrenoceptor knockout ($\alpha_{1B/D}$-KO) mesenteric and carotid arteries. Smooth muscle cells were outlined and measured as Regions of Interest. Imaging was performed at low power (zoom 3) for mesenteric arteries and high power (zoom 8) for carotid arteries. An image size of 512 × 512 pixels produced a field size of 96 × 96 μm for mesenteric arteries and 36 μm × 36 μm for carotid arteries.

Figure S3 Effect of 5-methylurapidil (5MeU) on contractile response to phenylephrine in mouse carotid arteries of $\alpha_{1B/D}$-adrenoceptor knockout (n = 6). Data points are expressed as percentage of control curve maximum as mean ± S.E.M.

Figure S4 Example images of BODIPY FL-Prazosin (QAPB) fluorescent binding on a plane imaged from the endothelial side (left image; average pixel intensity 78.3) and a plane imaged from the adventitial side (right image; average pixel intensity 77.7) from the same z-stack of a mesenteric artery. An image size of 512 × 512 pixels produced a field size of 96 μm × 96 μm.

Please note: Wiley-Blackwell are not responsible for the content or functionality of any supporting materials supplied by the authors. Any queries (other than missing material) should be directed to the corresponding author for the article.